

RESEARCH PAPER



## Targeting *LINC00673* expression triggers cellular senescence in lung cancer

Anna Roth<sup>a</sup>, Karine Boulay<sup>a</sup>, Matthias Groß<sup>a</sup>, Maria Polycarpou-Schwarz<sup>a</sup>, Frédérick A. Mallette<sup>b</sup>, Marine Regnier<sup>b</sup>, Or Bida<sup>c</sup>, Doron Ginsberg<sup>c</sup>, Arne Warth<sup>d,e</sup>, Philipp A. Schnabel<sup>d\*</sup>, Thomas Muley<sup>e,f</sup>, Michael Meister<sup>e,f</sup>, Heike Zabeck<sup>f</sup>, Hans Hoffmann<sup>g#</sup>, and Sven Diederichs<sup>g,a,h</sup>

<sup>a</sup>Division of RNA Biology & Cancer (B150), German Cancer Research Center (DKFZ), Heidelberg, Germany; <sup>b</sup>Chromatin Structure and Cellular Senescence Research Unit, Maisonneuve-Rosemont Hospital Research Centre & Department of Medicine, Université de Montréal, Montreal, Canada; <sup>c</sup>The Mina and Everard Goodman Faculty of Life Science, Bar Ilan University, Ramat Gan, Israel; <sup>d</sup>Institute of Pathology, University Hospital Heidelberg, Heidelberg, Germany; <sup>e</sup>Translational Lung Research Centre Heidelberg (TLRC-H), Member of the German Center for Lung Research (DZL), Heidelberg, Germany; <sup>f</sup>Thoraxklinik Heidelberg, Heidelberg, Germany; <sup>g</sup>Division of Cancer Research, Department of Thoracic Surgery, Medical Center - University of Freiburg, Faculty of Medicine, University of Freiburg, Freiburg, Germany; <sup>h</sup>German Cancer Consortium (DKTK), Freiburg, Germany

### ABSTRACT

Aberrant expression of noncoding RNAs plays a critical role during tumorigenesis. To uncover novel functions of long non-coding RNA (lncRNA) in lung adenocarcinoma, we used a microarray-based screen identifying *LINC00673* with elevated expression in matched tumor versus normal tissue. We report that loss of *LINC00673* is sufficient to trigger cellular senescence, a tumor suppressive mechanism associated with permanent cell cycle arrest, both in lung cancer and normal cells in a p53-dependent manner. *LINC00673*-depleted cells fail to efficiently transit from G1- to S-phase. Using a quantitative proteomics approach, we confirm the modulation of senescence-associated genes as a result of *LINC00673* knockdown. In addition, we uncover that depletion of p53 in normal and tumor cells is sufficient to overcome *LINC00673*-mediated cell cycle arrest and cellular senescence. Furthermore, we report that overexpression of *LINC00673* reduces p53 translation and contributes to the bypass of Ras-induced senescence. In summary, our findings highlight *LINC00673* as a crucial regulator of proliferation and cellular senescence in lung cancer.

### ARTICLE HISTORY

Received 12 November 2018  
Accepted 17 November 2018

### KEYWORDS

*LINC00673*; long noncoding RNA; lung cancer; p53; senescence

### Introduction

Lung cancer accounts for most of the cancer-related deaths worldwide and is associated with a poor prognosis [1]. The group of non-small cell lung cancer (NSCLC) represents 85% of diagnosed lung neoplasms with lung adenocarcinoma (ADC) being the most abundant subtype [2]. Comprehensive analyses revealed that over 80% of the human genome is transcribed and the class of long noncoding RNAs (lncRNA) accounts for a significant proportion of the noncoding transcriptome [3,4]. lncRNAs are generally defined to be longer than 200 nucleotides with little or no protein-coding potential [5]. In-depth analyses of the epigenetic, genomic and transcriptional landscape of human cancers revealed that many lncRNAs exhibit cancer type-specific aberrant expression [6], thus presenting a source of novel markers and alternative target molecules for cancer therapy [7]. lncRNAs play critical roles in the onset and progression of cancer [8–10], and various studies have confirmed their impact on epigenetic, transcriptional as well as post-transcriptional gene regulation [5]. To comprehensively understand lung cancer-promoting pathways and uncover potential novel druggable targets for cancer therapy, multiple screens for lncRNAs were conducted utilizing lung cancer specimens [9]. However, to date only few lncRNAs have been thoroughly characterized.

In this study, we identify the altered expression of 479 ncRNAs in lung ADC patient samples compared to normal tissue using a comparative microarray profiling approach. We characterize the most upregulated lncRNA *LINC00673* in functional detail and define its role in the regulation of cellular senescence, a state of stable cell cycle arrest which is recognized as an effective tumor suppressor mechanism [11].

### Results


#### *LINC00673* is upregulated in lung adenocarcinoma

To identify novel dysregulated ncRNAs, 27 early-stage lung ADC and adjacent non-malignant lung samples derived from patients, were subjected to a microarray-based expression profiling. 479 ncRNAs were differentially expressed between tumor and normal tissues with a significant and minimum twofold change (Fig. 1A, Suppl. Fig. S1, Suppl. Table S1). As a control for the validity of our microarray hybridization and analysis, we identified sex-specific expression patterns between normal or malignant lung tissues from male versus female patients (Suppl. Fig. S2A,B). Six mRNAs and one lncRNA, namely *XIST*, were independently identified as significantly differentially expressed between male and female patients (adjusted  $P < 0.05$  (FDR), fold change  $FC \geq 2$ ).

**CONTACT** Sven Diederichs  [s.diederichs@dkfz.de](mailto:s.diederichs@dkfz.de)

\*Present address: Saarland University Hospital, Institute of General and Special Pathology, Homburg/Saar, Germany

#Present address: Division of Thoracic Surgery, University Hospital rechts der Isar, Technical University of Munich, Munich, Germany

 Supplemental data for this article can be accessed [here](#).

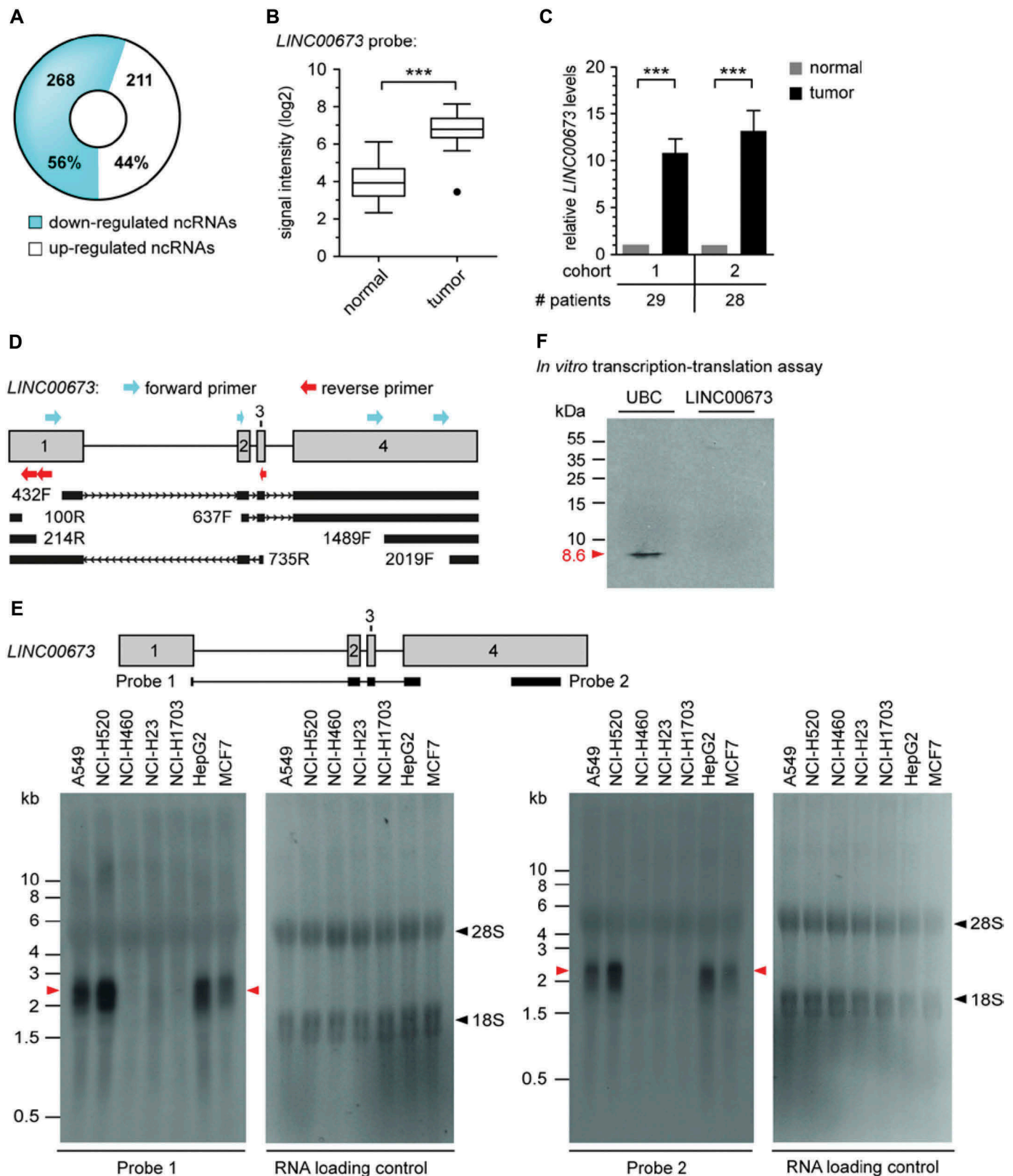


**Figure 1.** Identification, validation and characterization of *LINC00673* lncRNA. (A) Comparative microarray analysis identified 479 significantly deregulated ncRNAs in non-matched lung ADC vs. normal lung patient samples ( $n = 27$ , corrected  $P < 0.05$ ,  $FC \geq 2$ ). (B) *LINC00673* lncRNA expression was significantly enhanced in lung ADC ( $n = 27$ ; absolute FC between tumor and normal samples is shown, with \*\*\*,  $P < 0.001$ ). (C) Elevated *LINC00673* levels were validated by RT-qPCR analysis in two patient cohorts (cohort 1 overlapping with the microarray cohort) comprising matched tumor and normal samples. *PPIA* was used as reference gene and the mean ratios of tumor/normal (T/N) + SEM are shown. Statistical significance was determined with paired Student  $t$  test, with \*\*\*,  $P < 0.001$ . (D) Schematic overview of detected transcripts matching *LINC00673* reference sequence by RACE in A549 cDNA. The first nucleotide of each RACE primer is indicated (F: forward primer, R: reverse primer). (E) Northern Blot analysis of *LINC00673* in different cell lines. 18S and 28S rRNA bands are indicated by black arrows. (F) *In vitro* transcription-translation assay based on DNA templates. The incorporation of [<sup>35</sup>S] methionine into proteins was detected by autoradiography, and ubiquitin C (UBC) served as positive control. One representative experiment is shown ( $n = 3$ ).

Notably, the six male-specific transcripts were all derived from the Y chromosome while the one female-specific transcript was *XIST*, the lncRNA involved in inactivation of the second X chromosome in female cells. The results were identical when either normal or tumor tissues were analyzed separately demonstrating the reliability of the identified transcript signature. In agreement with previous reports, the majority of detected ncRNAs was less abundant compared to mRNAs [3,12] (Suppl. Fig. S3). The ncRNA *LINC00673* was the most significantly and most highly upregulated ncRNA in lung ADC using our comparative microarray analysis (Fig. 1B). We validated our microarray results by RT-qPCR in two independent patient cohorts (Fig. 1C, Suppl. Fig. S4) and identified *LINC00673* expression in multiple cancer cell lines derived from different tumors (Suppl. Fig. S5A). In addition, we used the TANRIC platform [13] to uncover the enhanced expression of *LINC00673* in various other malignancies (Suppl. Fig. S5B) supporting a potentially oncogenic role for this lncRNA. *LINC00673* expression did not correlate with patient survival, lung cancer stage or the smoking behavior in TCGA lung ADC (Suppl. Fig. S6A–C) suggesting a low prognostic and predictive value for lung ADC.

### Molecular characterization of *LINC00673*

We next established the full-length sequence of the *LINC00673* transcript by rapid amplification of cDNA ends (RACE) in the lung cancer cell line A549 (Fig. 1D) and by Northern blot (Fig. 1E). The transcript comprised of 4 exons

and a length of roughly 2.3 kb coinciding with the database sequence of *LINC00673* (NR\_036488). Notably, the detected Northern blot signal intensities for *LINC00673* positively correlated with the determined relative expression of *LINC00673* using RT-qPCR in selected cell lines (Suppl. Fig. S5A). We further examined the coding potential of *LINC00673* by conducting a search for putative open reading frames (ORF) using the NCBI ORF Finder tool. A total of six putative ORFs were identified, of which five matched the canonical AUG start codon (data not shown). None of the predicted peptides were identified in the deposited tandem mass spectrometry data provided by PeptideAtlas [14]. Further supporting the noncoding nature of *LINC00673*, an *in vitro* translation approach failed to generate detectable proteins from a DNA template, while the ubiquitin C (UBC) control protein was efficiently produced (Fig. 1F).

The determination of the subcellular localization of a lncRNA might provide critical information about its biological functions [15]. Hence, cellular fractionation experiments of A549 cells revealed an enrichment of *LINC00673* in the cytoplasm (Fig. 2A), which was further confirmed by RNA FISH (fluorescence *in situ* hybridization; Fig. 2B). Moreover, we examined the half-life of *LINC00673* by measuring the relative abundance of transcripts in actinomycin D-treated A549 cells by RT-qPCR (Fig. 2C). *LINC00673* displayed a short half-life of <2 h, which is characteristic of known regulatory RNAs [16]. The stable housekeeping mRNA *PPIA* [16] and the rapidly processed 45S pre-rRNA were used as controls.

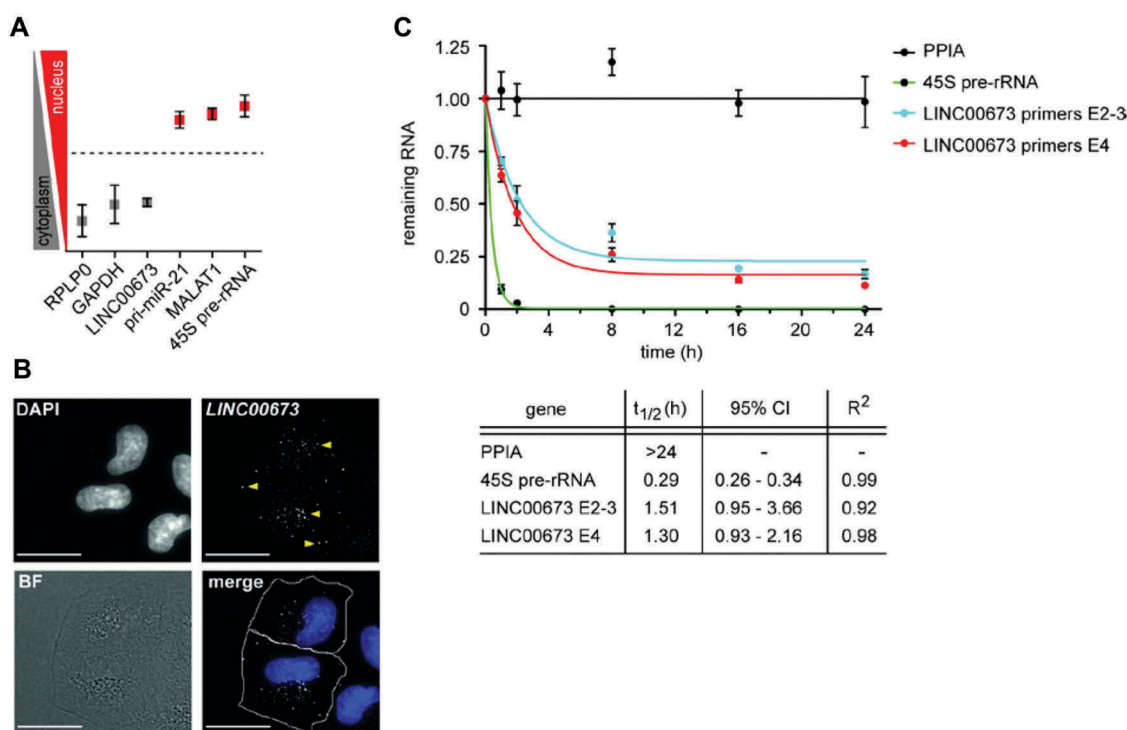


**Figure 2.** *LINC00673* is a cytoplasmic lncRNA with a short half-life. (A) Cellular fractionation of A549 cells and subsequent RT-qPCR (represented as nuclear/cytoplasmic (log<sub>2</sub>) ratios) indicated an enrichment of *LINC00673* in the cytoplasmic fraction. Data represent the mean  $\pm$  SEM ( $n = 3$ ). (B) RNA FISH using custom Stellaris (LGC Biosearch Technologies) probes for *LINC00673* revealed a cytoplasmic localization. Yellow arrows indicate lncRNA signal, and the scale bars represent 20  $\mu$ m. BF: brightfield. (C) RNA stability was determined by actinomycin D (10  $\mu$ g/ml) treatment of A549 cells for up to 24 h and the RNA levels were measured by RT-qPCR. *LINC00673* expression was detected with two different primer pairs spanning exon 2–3 (E2-3) and located within exon 4 (E4), respectively. Data represent the mean  $\pm$  SEM ( $n = 3$ ),  $t_{1/2}$ : half-life, CI: confidence interval. Data was fitted to a non-linear least squares regression curve (one phase decay) with GraphPad Prism 5.

## **LINC00673 is a regulator of cell proliferation**

As a first step to approach the possible function of *LINC00673* in lung cancer, we sought to analyze commonalities with genes whose expression correlated with *LINC00673* lncRNA in the TCGA lung ADC set using the TANRIC platform. Subsequent functional profiling of positively correlated genes with g:Profiler [17] revealed a striking enrichment of E2F-regulated genes (transcription factor binding sites are retrieved from TRANSFAC database, Suppl. Fig. S7A). In addition, levels of *LINC00673* and E2F1 protein significantly correlated in different lung fibroblast and lung cancer cell lines (Suppl. Fig. S7B,C,D, Suppl. Table S2). Implicating *LINC00673* in the same pathway by guilt-by-association, the putative *LINC00673* promoter region itself was recognized by E2F1 according to publically available ChIP-Seq data (Suppl. Fig. S7E). To investigate whether E2F1, an important regulator of cell cycle progression [18], also regulated the expression of *LINC00673*, we took advantage of the human lung cancer cell line NCI-H1299 and the human embryonic lung fibroblasts WI-38 stably expressing conditionally active E2F1, namely ER-E2F1 [19]. The activation of ER-E2F1 by 4-hydroxytamoxifen (OHT) significantly increased *LINC00673* expression in both cell lines (Suppl. Fig. S7F). In support of a direct regulation of *LINC00673* levels, the activation of ectopic E2F1 in the presence of the protein synthesis inhibitor cycloheximide (CHX) still led to the induction of *LINC00673* (Suppl. Fig. S7G). To investigate whether *LINC00673* levels were also regulated during the cell cycle, IMR-90 normal immortalized human lung fibroblast cells as well as A549 lung adenocarcinoma cells were arrested in G0 by serum starvation and transcript levels measured after releasing the cells from the cell cycle block. In the normal fibroblasts, *E2F1* and its known target gene *MCM6* [20] were induced, while *LINC00673* levels were not regulated in a cell cycle-dependent manner (Suppl. Fig. S7H). In the lung cancer cells, *LINC00673*, *E2F1* and *MCM6* RNA levels correlated well with each other showing a decrease upon serum starvation and an increase upon release from starvation (Suppl. Fig. S7I). We concluded that endogenous E2F1 did not regulate *LINC00673* during normal cell cycle progression, but that aberrant E2F1 activity in transformed cells lead to elevated *LINC00673* levels. Given the correlation of *LINC00673* with E2F-regulated cell cycle-associated genes at steady state levels, we sought to investigate whether *LINC00673* itself was a crucial regulator of cell proliferation.

To explore the cellular functions of *LINC00673*, we conducted knockdown studies by applying two different knockdown tools, namely LNA longRNA GapmeRs (Exiqon) and siPOOLS (siTOOLS Biotech). The latter comprise a well-defined, custom-designed pool of 30 siRNAs targeting the gene of interest and were previously shown to eliminate off-target effects that are frequently observed with single siRNAs [21]. Knockdown efficiency of *LINC00673* in the lung cancer cell lines A549 and Calu-3 was confirmed using either GapmeRs or the siPOOL (Suppl. Fig. S8A,B). Depletion of *LINC00673* using either GapmeRs or the siPOOL significantly decreased A549 cell number (Fig. 3A). This effect was not caused by an increased apoptotic response since no significantly enhanced activation of

the cellular caspases 3 and 7 was observed (Fig. 3B). To investigate whether the decrease in cell number was a result of reduced cell proliferation, we quantified the incorporation of BrdU 24 h and 48 h after *LINC00673* knockdown, respectively. The GapmeR- and siPOOL-mediated knockdown of *LINC00673* both significantly decreased cell proliferation of A549 and Calu-3 cells (Fig. 3C). Notably, *LINC00673* knockdown also reduced cell proliferation of the normal human lung fibroblasts WI-38 and IMR-90 (Fig. 3D). The described observations were consistent with GapmeR- and siPOOL-mediated knockdown of *LINC00673* in lung cancer cells. Discrepancies in the strength of monitored effects were mainly observed between the two GapmeRs and pointed towards possible off-target effects despite comparable knockdown efficiencies (Fig. 3A). For this reason, siPOOL-mediated knockdown of *LINC00673* was used in all subsequent experiments.

The reduction of *LINC00673* levels in A549 cells was accompanied by a prominent increase of cells in G0/G1-phases and a concomitant decrease of cells in S-phase (Fig. 3E). Moreover, we found that *LINC00673*-depleted IMR-90 cells arrested in G0/G1 were unable to re-enter the cell cycle efficiently and consequently displayed a strong reduction in proliferation after serum stimulation (Fig. 3F). We confirmed an efficient knockdown of *LINC00673* in starved IMR-90 cells and additionally were able to show a diminished induction of *E2F1* and *MCM6* upon cell cycle re-entry as compared to the siPOOL control condition (Suppl. Fig. S8C). In accordance with our experimental data, we uncovered a highly significant enrichment of *LINC00673*-correlated genes in the gene ontology terms of mitotic cell cycle and cell cycle phase transition (Suppl. Fig. S9). Thus, loss of *LINC00673* severely impaired cell cycle progression.

## **LINC00673 depletion triggers cellular senescence**

*LINC00673* knockdown caused a change of cellular morphology, namely increased cell size and adaptation of a flat cell morphology in both A549 lung cancer cells and IMR-90 normal lung fibroblast cells (Suppl. Fig. S10). These alterations are morphological hallmarks of cellular senescence [22], a state of stable proliferative arrest.

In response to various stimuli, cellular senescence is controlled by the tumor suppressor pathways p16<sup>INK4a</sup>/pRb and p53 [22,23]. Noteworthy, disruption of the pRb and the p53 pathways is frequent in NSCLC [24–26]. The experimental cell models used here reflect these different genetic backgrounds. A549 cells present a homozygous deletion of the p16<sup>INK4a</sup>/p14<sup>ARF</sup> locus, whereas IMR-90 lung fibroblasts employ functional pRb and p53 pathways.

Numerous senescence markers have been proposed and their occurrence partially depends on cell and tissue types [27]. We chose to first analyze the accumulation of senescence-associated  $\beta$ -galactosidase (SA- $\beta$ -Gal) [28] and the decreased expression of E2F1 target genes [29–32] as indicators of senescence. We confirmed a strong increase of SA- $\beta$ -Gal positive A549 and IMR-90 cells 4 days after *LINC00673* knockdown (Fig. 4A,B). Doxorubicin treatment of cells served as a positive control for SA- $\beta$ -Gal stainings. Next, we investigated the expression of

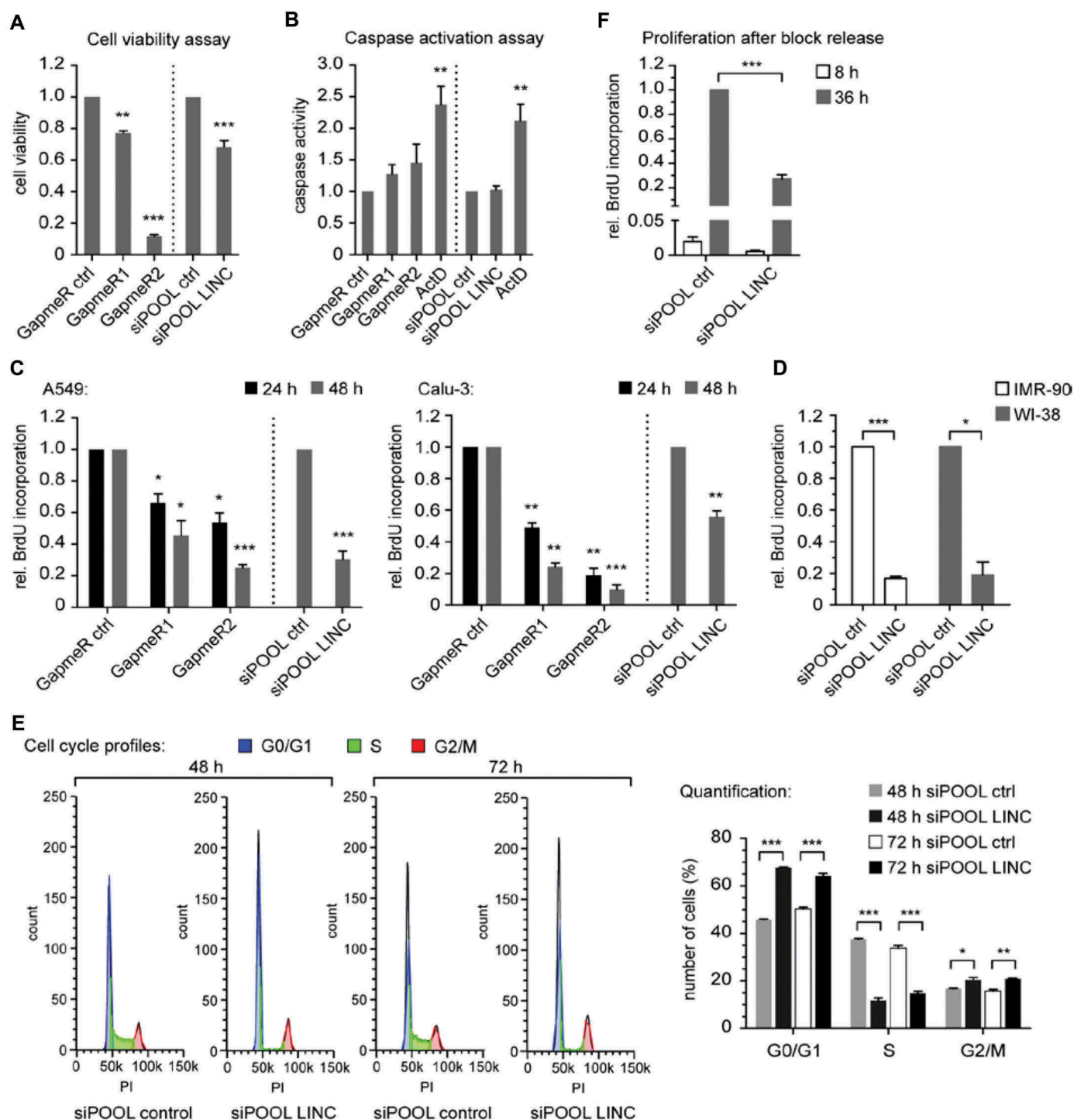


**Figure 3.** *LINC00673* reduces cell proliferation and induces a cell cycle arrest. (A) CellTiter-Glo Luminescent Cell Viability Assay (Promega) was performed 48 h after *LINC00673* knockdown in A549 cells with GapmeRs (60 nM;  $n = 3$ ) and siPOOLS (10 nM;  $n = 4$ ), respectively. (B) Caspase-Glo 3/7 luminescent assay (Promega) was performed 24 h after *LINC00673* knockdown in A549 cells (final concentration of GapmeRs and siPOOLS as in A;  $n = 6$  for GapmeR-mediated knockdown and  $n = 4$  for siPOOL-mediated knockdown experiments). Treatment with actinomycin D (ActD; 5  $\mu\text{g}/\text{ml}$ ) served as a positive control for apoptosis induction. (C) BrdU Cell Proliferation ELISA Kit (Roche) was used to quantify cell proliferation 24 h and 48 h after *LINC00673* knockdown (final concentrations as in A;  $n = 3$  for GapmeR-mediated knockdown in A549 and Calu-3;  $n = 5$  for siPOOL-mediated knockdown in A549 and  $n = 3$  for Calu-3). (D) BrdU Cell Proliferation ELISA Kit was used to quantify cell proliferation 48 h after siPOOL-mediated knockdown (final concentration of 1 nM) of *LINC00673* in IMR-90 and WI-38 cells ( $n = 3$ ). (E) Cell cycle profiles of A549 cells were analyzed by FACS after 48 h and 72 h of *LINC00673* knockdown. Quantification of cells with the cell cycle function of FlowJo (V10) and the cell cycle profiles of one representative experiment are shown ( $n = 3$ ). (F) IMR-90 cells were serum starved for 24 h and subsequently transfected with 0.3 nM siPOOLS. Cells were released by adding complete medium supplemented with 10% FBS at 72 h after knockdown and BrdU incorporation was measured 8 h and 36 h following block release ( $n = 4$ ). In A-F the mean + SEM is shown and the statistical significance was determined per two-sided unpaired Student  $t$  test, with \*,  $P < 0.05$ ; \*\*,  $P < 0.01$ ; \*\*\*,  $P < 0.001$ .

E2F-regulated genes and crucial cell cycle regulators following *LINC00673* knockdown [20]. Significant reduction of selected genes became evident at the transcript level in A549 cells as

soon as 48 h following depletion (Fig. 4C), an early timepoint undergoing cell cycle arrest (Fig. 3E). Furthermore, we noted the elevated expression of genes characteristic for the senescence-

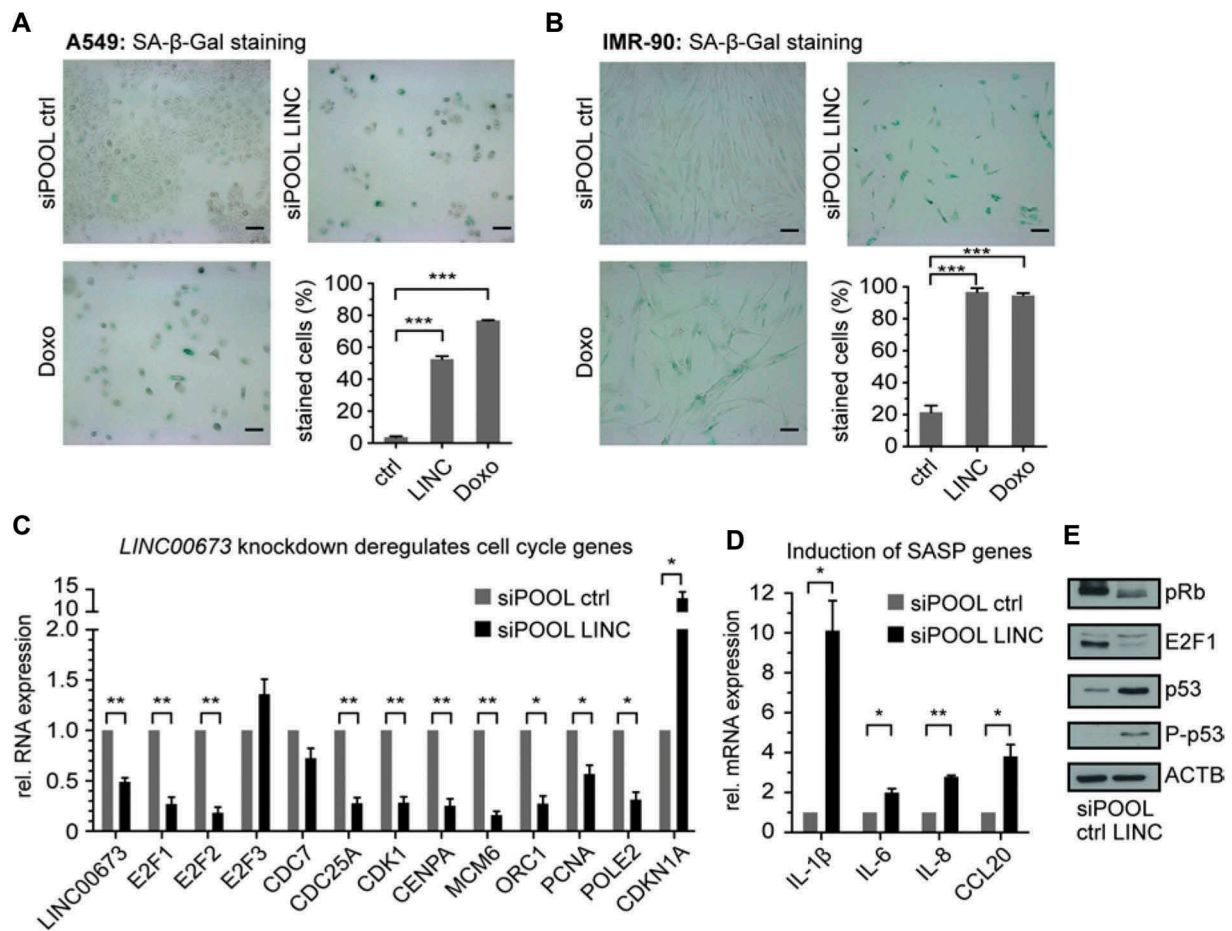


**Figure 4.** *LINC00673* depletion induces a senescence-like phenotype. (A) SA-β-Gal accumulated in A549 cells 4 days after *LINC00673* knockdown with siPOOLS (3 nM). As a positive control for staining, cells were treated with 200 nM doxorubicin. At least 200 cells were counted per condition ( $n = 4$ ). The scale bar represents 100  $\mu$ m. (B) SA-β-Gal staining of IMR-90 cells as in A ( $n = 3$ ). (C) Cell cycle and E2F-regulated genes were determined by RT-qPCR at 48 h after *LINC00673* knockdown with siPOOLS (3 nM) in A549 cells. *GAPDH* was used as reference gene ( $n = 3$ ). (D) SASP gene expression in A549 cells was determined by RT-qPCR as in C ( $n = 3$ ). (E) Western Blot analysis 48 h after *LINC00673* knockdown with siPOOLS (3 nM) in A549 cells. Specific antibodies were used for indicated proteins. One representative Western Blot is shown ( $n = 3$ ). All data is shown as mean + SEM and the statistical significance was determined per two-sided unpaired Student *t* test, with \*,  $P < 0.05$ ; \*\*,  $P < 0.01$ ; \*\*\*,  $P < 0.001$ .

associated secretory phenotype (SASP) [33] in A549 cells (Fig. 4D) and IMR-90 cells (Suppl. Fig. S11A, B).

The senescence-associated cell cycle exit was previously linked to the formation of facultative heterochromatin foci at E2F-responsive promoters, a process that is mediated by pRb [32]. IMR-90 cells contain a functional p16<sup>INK4a</sup>/pRb pathway and therefore displayed enhanced formation of H3K9me3-positive foci, a surrogate marker of the senescence-associated heterochromatin foci (SAHF) phenotype (Suppl. Fig. S12). Also, *LINC00673* depletion-mediated senescence was not primarily caused by persistent DNA damage since we were unable to detect the accumulation of  $\gamma$ -H2AX foci 4 days after *LINC00673* knockdown [34–36] (Suppl. Fig. S12).

Depletion of E2F1 in cancer cells was previously linked to the induction of senescence independent of the pRb and p53 status of the cell line [37]. We also noted a decrease of E2F1 transcript and protein levels upon *LINC00673* knockdown in A549 cells (Fig. 4C,E). Simultaneously, the accumulation and activation of p53 and the elevated expression of p21 underlined the potential contribution of the p53 pathway in establishing the *LINC00673* depletion-mediated senescence phenotype (Fig. 4E). Although we were unable to detect

persistent DNA damage foci in senescent cells, the occurrence of phospho-p53<sup>S15</sup> suggested that the DNA damage signaling pathway contributed, at least partially, to the onset of the phenotype [34–36]. In addition, we noted an increase in hypophosphorylated pRb in A549 cells (Fig. 4E), which was in agreement with a previous report on DNA damage-induced senescence in PC-3 prostate cancer cells [37]. In summary, we concluded that the *LINC00673* depletion-mediated senescence phenotype might engage the p53 pathway but did not require p16<sup>INK4a</sup> activity and was not a direct cause of persistent DNA damage.

#### **LINC00673 depletion-induced senescence relies on the p53 pathway**

We sought to analyze in more detail whether the cell cycle arrest upon *LINC00673* depletion is a consequence of p53 or pRb pathway activation. For this purpose, we quantified the ability of A549 and IMR-90 cells to proliferate following simultaneous knockdown of *LINC00673*, p53 and/or pRb. The loss of p53 was sufficient to rescue the proliferation defect in both A549 and IMR-90 cells (Fig. 5A,B). In contrast, pRb

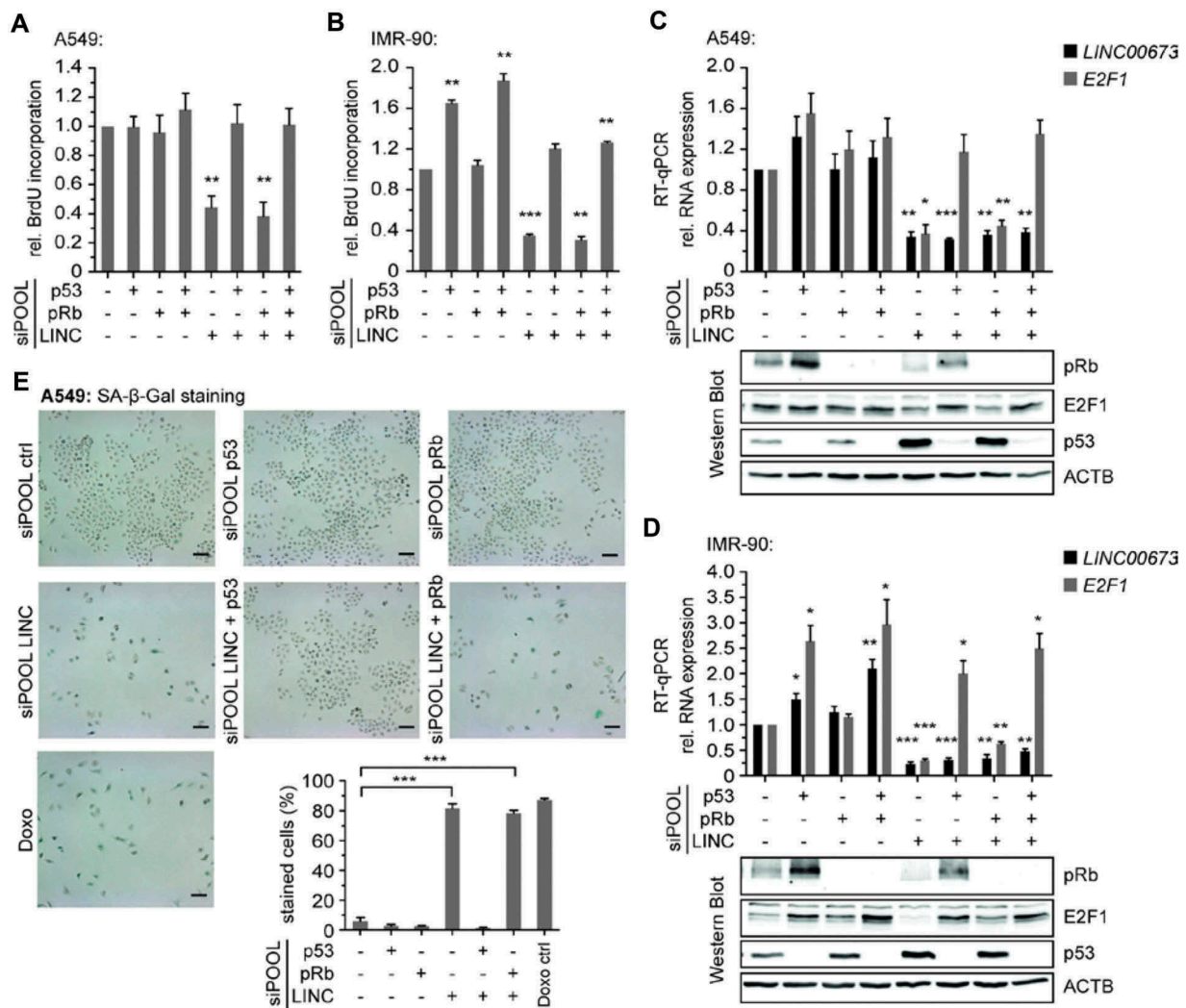


**Figure 5.** *LINC00673*-mediated senescence is p53-dependent. (A) BrdU Cell Proliferation ELISA Kit was used to quantify cell proliferation 48 h after knockdown of p53, pRb and *LINC00673* in A549 ( $n = 4$ ). The reactions contained siPOOL negative control (12 nM) or a mix of 1 nM siPOOL p53, pRb and 10 nM siPOOL *LINC00673* supplemented with siPOOL negative control for a final concentration of 12 nM. (B) BrdU incorporation in IMR-90 cells was measured as in A. The reactions contained siPOOL negative control (0.9 nM) or a mix of 0.3 nM siPOOL p53, pRb and *LINC00673* supplemented with siPOOL negative control for a final concentration of 0.9 nM. (C) Relative RNA levels were determined by RT-qPCR at 48 h after knockdown in A549 cells ( $n = 3$ ). The reactions contained siPOOL negative control (5 nM) or a mix of 1 nM siPOOL p53, pRb and 3 nM siPOOL *LINC00673* supplemented with siPOOL negative control for a final concentration of 5 nM. *GAPDH* was used as reference gene. One representative Western Blot is shown ( $n = 3$ ). (D) RT-qPCR as in C using IMR-90 cells ( $n = 4$ ). The siPOOL concentrations were as described in B. One representative Western Blot is shown ( $n = 4$ ). (E) SA-β-Gal accumulated in A549 cells 4 days after knockdown. The reactions contained siPOOL negative control (4 nM) or a mix of 3 nM siPOOL *LINC00673* and 1 nM siPOOL p53 or pRb supplemented with siPOOL negative control for a final concentration of 4 nM ( $n = 4$ , scale bar = 100 μm). In A-E, the mean + SEM is shown. The statistical significance was determined per two-sided unpaired Student *t* test, with \*,  $P < 0.05$ ; \*\*,  $P < 0.01$ ; \*\*\*,  $P < 0.001$ .

depletion did not restore cell proliferation. The ability to proliferate positively correlated with E2F1 levels, which could only be restored and induced upon p53 depletion in A549 and IMR-90 cells, respectively (Fig. 5C,D). Active p53 protein was necessary to establish the cell cycle arrest as monitored by the specific accumulation of p53 and the increase in *CDKN1A* transcript levels (Fig. 5C,D, Suppl. Fig. S13). We confirmed that the knockdowns were efficient in all conditions both on RNA and protein levels (Fig. 5C,D, Suppl. Fig. S13). Finally, the siPOOL-mediated depletion of p53 was sufficient to overcome senescence triggered by *LINC00673* depletion in A549 cells (Fig. 5E).

Since activating mutations of Ras [38] and elevated expression of *LINC00673* (Fig. 1) constitute frequent events in lung cancer, we determined whether ectopic expression of *LINC00673* can contribute to the bypass of Ras-induced senescence. In human

lung fibroblasts, activated Ras engages both the p53 and pRb pathways, and these two pathways need to be inactivated in order to bypass Ras-induced senescence [39,40]. While the sole expression of *LINC00673* was not sufficient to bypass Ras-induced senescence, combined expression of *LINC00673* and inactivation of the pRb pathway using E7 from the human papillomavirus (HPV) type 16 significantly abrogated the senescence response (Suppl. Fig. S14). On the other hand, expression of *LINC00673* in p53-inactivated cells using the HPV E6 oncoprotein had no impact on senescence entry upon Ras expression (Suppl. Fig. S14). These results suggested that elevated levels of *LINC00673* contribute to the bypass of Ras-induced cellular senescence by inactivating the p53 pathway, and could thus play a critical role during tumorigenesis.

To verify our findings and monitor alterations in protein expression at an early timepoint, namely 48 h following

*LINC00673* knockdown in A549 cells, we chose an unbiased quantitative mass spectrometry approach using SILAC. Thereby, we identified a total of 20 up- and 12 downregulated proteins in comparison to the siPOOL control condition (biological duplicate, *t* test with  $P < 0.05$ , fold change  $>1.5$ , Fig. 6A, Suppl. Table S3, Suppl. Fig. S15). We validated our results by RT-qPCR and confirmed that the majority of the modulated proteins displayed altered mRNA levels (Suppl. Fig. S16A,B). Interestingly, 50 % (10 out of 20) of the identified upregulated proteins were direct targets of p53, while 47 % (15 out of 32) of all identified proteins were previously associated with cellular senescence (Suppl. Table S4). Specifically, we identified the upregulation of the p53 targets and known senescence regulators PAI-1 [41] and DDB2 [42]. Among the proteins with reduced abundances, we detected UHRF1 and PRC1. While UHRF1 is known to negatively regulate the tumor suppressors p16<sup>INK4A</sup>, hMLH1, p21, pRb

and PML [43], reduced PRC1 levels were previously observed in oncogenic Ras-induced and replicative senescence [44]. We found that p53 knockdown was able to at least partially restore the gene expression of selected SILAC hits (Suppl. Fig. S17). Overall, the deregulation of identified genes is in line with the early induction of a senescence phenotype in A549 cells.

We further analyzed whether the knockdown of UHRF1 would be sufficient to reduce cell proliferation of IMR-90 normal human lung fibroblasts. We confirmed an efficient knockdown by siPOOL both on protein and mRNA level (Fig. 6B, Suppl. Fig. S18A), and noted a reduction in BrdU incorporation (Fig. 6C). This effect was further significantly enhanced by simultaneous *LINC00673* knockdown suggesting a relevant role for UHRF1 in cell cycle progression in IMR-90 cells. Since PAI-1 is a critical downstream target of p53 for the induction of replicative senescence in primary fibroblasts [41], we investigated the influence of

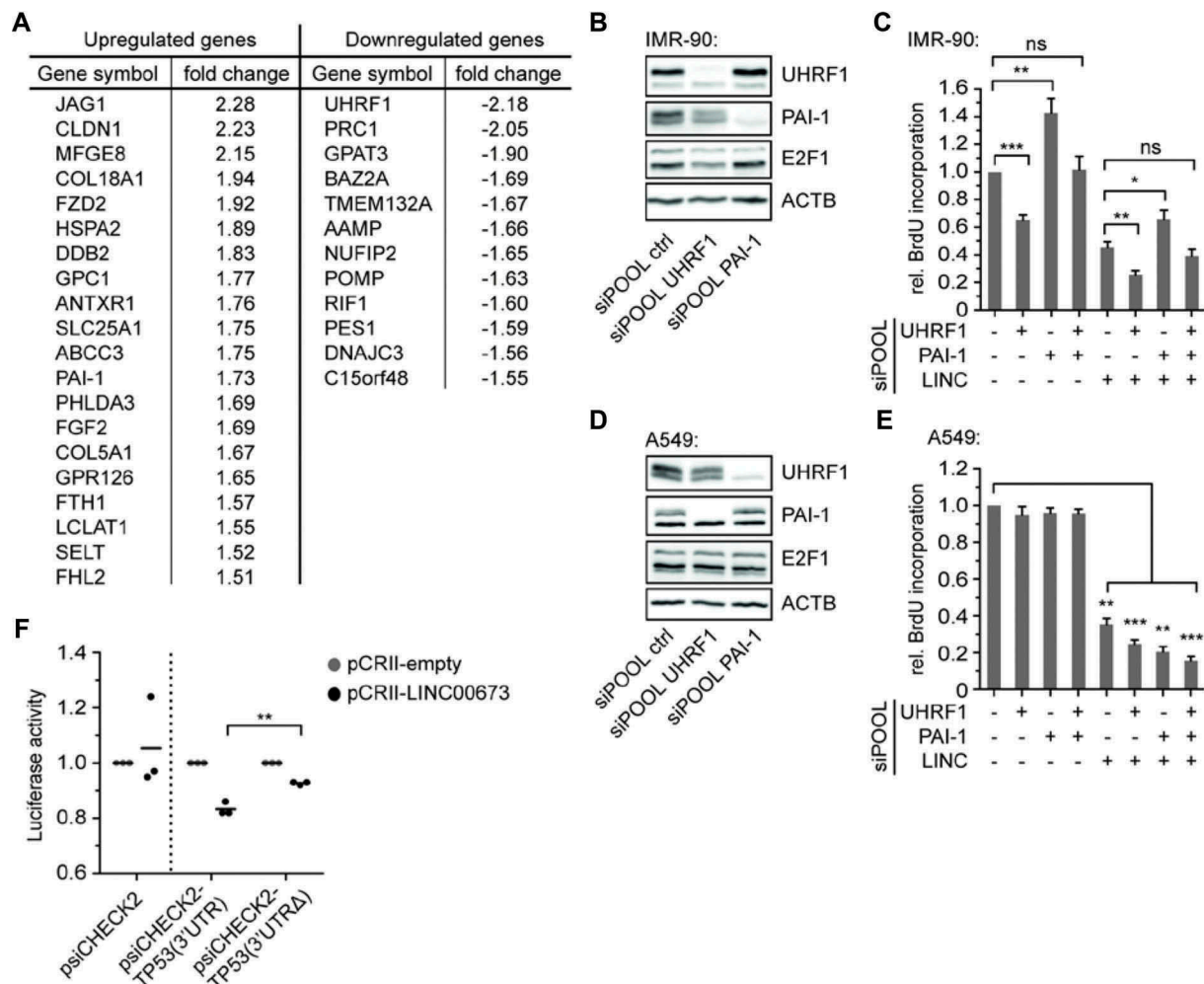


**Figure 6.** *LINC00673* acts by regulating p53 translation. (A) A549 cells were adapted to SILAC medium and total protein lysates were prepared at 48 h following siPOOL-mediated knockdown of *LINC00673*. The lysates were analyzed by mass spectrometry and proteins that displayed an absolute fold change  $>1.5$  as compared to the siPOOL control are listed ( $n = 2$ , *t* test with  $P < 0.05$ ). (B) Protein levels were determined with specific antibodies 48 h after UHRF1 and PAI-1 knockdown with siPOOLS (final concentration of 0.3 nM) in IMR-90 cells. One representative Western Blot is shown ( $n = 3$ ). (C) Cell proliferation was quantified by BrdU incorporation at 48 h after knockdown of UHRF1, PAI-1 and *LINC00673* in IMR-90 ( $n = 7$ ). The reactions contained siPOOL negative control (0.9 nM) or a mix of 0.3 nM siPOOL UHRF1, PAI-1 supplemented with siPOOL negative control for a final concentration of 0.9 nM. (D) Protein expression was monitored at 48 h after UHRF1 and PAI-1 knockdown with siPOOLS (final concentration of 1 nM) in A549 cells. One representative Western Blot is shown ( $n = 3$ ). (E) Cell proliferation was quantified in A549 cells as described in C ( $n = 3$ ). The reactions contained siPOOL negative control (12 nM) or a mix of 1 nM siPOOL UHRF1, PAI-1 supplemented with siPOOL negative control for a final concentration of 12 nM. (F) Luciferase assays were performed in quadruplicates for each sample at 48 h after Hek293 transfection of a 1:5 ratio of psiCHECK2 and pCRII plasmids ( $n = 3$ ). In A-E, the mean + SEM is shown. The statistical significance was determined per two-sided unpaired Student *t* test, with \*,  $P < 0.05$ ; \*\*,  $P < 0.01$ ; \*\*\*,  $P < 0.001$ .



PAI-1 knockdown on IMR-90 cell proliferation. Indeed, the efficient reduction of PAI-1 levels by siPOOL (Fig. 6B, Suppl. Fig. S18A) increased BrdU incorporation and partially rescued the reduction of cell proliferation by *LINC00673* knockdown in IMR-90 cells (Fig. 6C). In contrast to our observations in IMR-90 cells, neither UHRF1 nor PAI-1 knockdown significantly affected A549 cell proliferation (Fig. 6D,E, Suppl. Fig. S18B). Noteworthy, neither UHRF1 nor PAI-1 knockdown significantly altered *LINC00673* levels, and UHRF1 knockdown reduced *E2F1* levels only in IMR-90 cells (Suppl. Fig. S18A, B). Together, these findings indicate that *LINC00673* depletion-mediated senescence, especially in lung cancer cells, is not established by a single downstream effector but rather by a more complex network of cellular responses depending on the activation of the p53 pathway.

In a recent study, direct interactions between the 7SL RNA and the 3'-untranslated region (UTR) of *TP53* mRNA were linked to reduced p53 translation [45]. We noted that *LINC00673* contained an Alu sequence (nucleotides 902–1217) displaying reverse complementarity to the *TP53* 3'UTR. We therefore hypothesized that *LINC00673* may negatively regulate p53 translation by directly interacting with the *TP53* 3'UTR, using a similar mechanism as the 7SL RNA. In analogy to a previous study by Abdelmohsen *et al.* [45], we cloned the *TP53* 3'UTR (nucleotides 1421–2591) into the psiCHECK2 dual luciferase vector [psiCHECK2-*TP53*(3'UTR)]. Additionally, we generated a psiCHECK2-*TP53*(3'UTRΔ) plasmid lacking the *LINC00673* interaction region. In Hek293 cells co-transfected with pCII-LINC00673 and psiCHECK2-*TP53*(3'UTR), luciferase activity was significantly reduced as compared to the psiCHECK2-*TP53*(3'UTRΔ) (Fig. 6F). As a control, luciferase activity was not

significantly altered after co-transfection of empty psiCHECK2 plasmid with pCII and pCII-LINC00673, respectively (Fig. 6F). In summary, our data indicate that the enhanced expression of *LINC00673* in lung cancer promotes cell proliferation by negatively regulating p53 expression and thereby confers resistance to senescence, which is a potent anti-tumor barrier (Fig. 7).

## Discussion

In this study, we show the elevated expression of lncRNA *LINC00673* or *linc00673* in lung ADC patient samples compared to normal surrounding tissue, which is in agreement with previous reports in NSCLC [46–48]. Elevated *LINC00673* levels were also described in melanoma [49], tongue squamous cell carcinoma [50] and gastric cancer [51,52], and found in other types of human cancers including breast, liver and thyroid cancer (Suppl. Fig. S5B).

Along with our data, recent studies about *LINC00673* function in lung cancer agree on a role in cell proliferation but not apoptosis [47,48]. More precisely, our results indicate that *LINC00673* depletion provokes a strong G1-phase arrest culminating in cellular senescence in lung cancer cells. One central property of tumor cells, cell cycle progression, is controlled by E2F transcription factors [18]. The multifunctional transcription factor E2F1 participates in the timely regulation of replication genes to promote G1/S transition, and has previously been shown to regulate the expression of various lncRNAs [19,53–56]. We provide evidence that E2F1 could elevate *LINC00673* levels in tumor cells. Interestingly, E2F1 was attributed a role in senescence regulation [57,58]. In

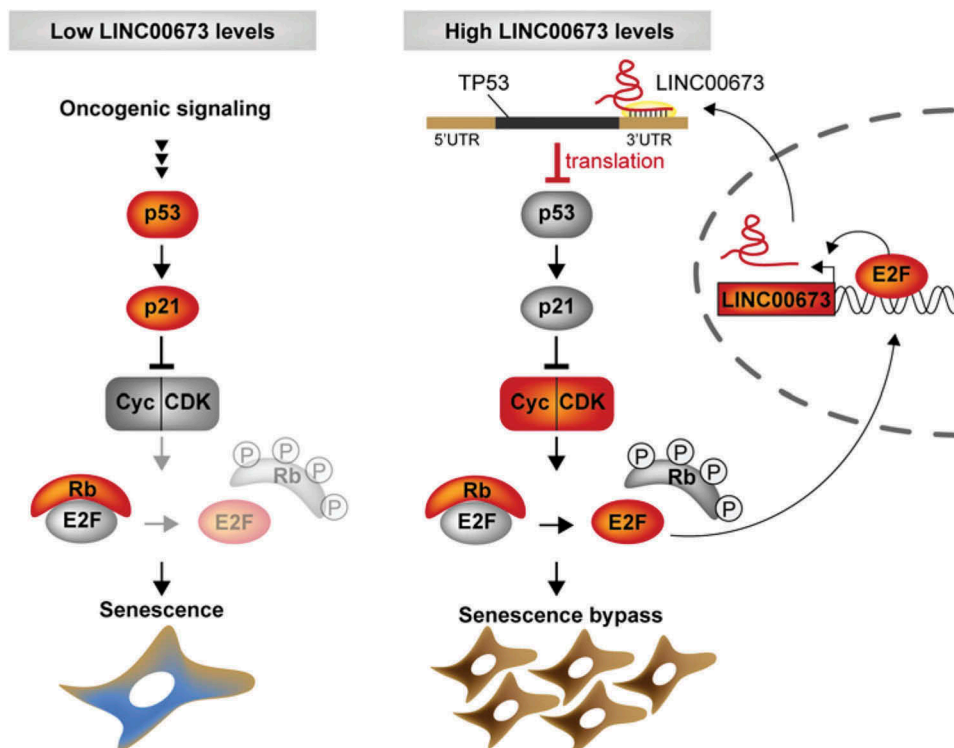


**Figure 7.** Schematic model of *LINC00673*-mediated senescence bypass in lung ADC. Constitutive mitogenic signaling e.g. by oncogenic Ras triggers p53 accumulation and activation resulting in cell cycle arrest and cellular senescence. In lung cells overexpressing oncogenic *LINC00673*, *TP53* translation is reduced by direct interactions between the *TP53* 3'UTR and *LINC00673*. Consequently, p53-mediated cell cycle arrest is abrogated leading to bypass of cellular senescence.

cancer cell lines, E2F1 depletion was sufficient to promote cellular senescence [37] and consequently, E2F1-responsive genes were downregulated [20,31,59]. With regard to *LINC00673*, we show that the depletion-mediated G1-phase arrest is also accompanied by reduced E2F1 and E2F-target levels.

Cellular senescence is a potent barrier against tumorigenesis *in vivo* [60–63], and hence, the discovery of novel regulators of senescence provides alternative cancer treatment options for the future [58]. Insights into the functional role of nuclear lncRNAs in the induction and maintenance of senescence were gained from studies that were mainly conducted in human fibroblast cells, and underlined the importance of nuclear lncRNAs in regulating senescence-associated gene signatures [64–66]. We show that a large fraction of *LINC00673* transcripts is localized in the cytoplasm, which is in line with recent reports in lung, pancreatic and gastric cancer [47,52,67]. Shi et al. proposed that *LINC00673* controls lung cancer cell proliferation by directly interacting with the H3K4 histone demethylase LSD1 and epigenetically silencing NCALD [47]. In our study, *LINC00673* knockdown does not cause extensive SAHF formation in lung cancer cell lines, which argues against a major role in epigenetic gene silencing in cellular senescence. The execution of the *LINC00673* depletion-mediated cellular senescence program does not require pRb action in cancer cells. Since p53 has been shown to induce cellular senescence by selectively cooperating with Rb2/p130 [68], Rb2 contribution in p16<sup>INK4a</sup>-proficient cells should also be investigated in further studies. However, our data clearly shows the importance of the p53-p21 pathway in *LINC00673* depletion-mediated cellular senescence as well as Ras-induced senescence.

We hypothesized that, by virtue of its cytosolic localization, *LINC00673* could act as a post-transcriptional regulator of senescence-inducing target genes. With regard to the mechanism, the ncRNAs *HULC*, *PTENP1* and *linc-MD1* were proposed to act as competing endogenous RNAs (ceRNA) that regulate their target genes post-transcriptionally by competing for the same set of miRNAs [69]. Recently, *LINC00673* has been shown to promote TGF- $\beta$ -induced EMT in NSCLC by sponging miR-150-5p and thereby enabling ZEB1 accumulation [48]. Other lncRNAs were implicated in the regulation of mRNA stability [70,71], decay [72,73] or mRNA translation [74–76]. Altogether only few senescence-associated cytoplasmic lncRNAs have been described to date [66]. Interestingly, reduction of 7SL RNA caused senescence by promoting p53 translation [45]. In analogy, we demonstrate a reduction in p53 translation by direct interaction between *LINC00673* (nucleotides 902–1217) and *TP53* 3'-UTR. The regulatory function of *LINC00673* is reinforced by its short half-life. We identified a number of additional dysregulated proteins following *LINC00673* depletion using a proteomics approach. Further studies are necessary to more precisely define further factors involved in p53 translational suppression, and investigate whether the proposed mechanism of post-transcriptional gene regulation by *LINC00673* can be extended to other proteins. Nuclear *LINC00673* could additionally engage in epigenetic regulation of target genes by associating with LSD1 and EZH2 in lung cancer [47,77]. In gastric cancer, a similar mode of action for oncogenic *LINC00673* was described, where direct interactions with LSD1 and EZH2

promoted repression of *KLF2* and *LATS2* gene expression [51], and *LINC00673* association with EZH2 and DNMT1 epigenetically silenced the tumor suppressor *KLF4* [52]. In a comprehensive study, Zheng et al. uncovered that the G > A variation at rs11655237 in *LINC00673* conferred susceptibility to pancreatic ductal adenocarcinoma in Han Chinese by creating a binding site for miR-1231 interfering with *LINC00673*-assisted PTPN11 degradation [67].

In pancreatic cancer, *LINC00673* transcript levels were reduced [67] indicating that *LINC00673* can exert oncogenic or tumor suppressive functions depending on the investigated tissue or cell type. Therefore, it is expected that *LINC00673* employs various different modes of action across different types of cancer. We suggest that enhanced *LINC00673* expression in early lung ADC contributes to lung tumorigenesis by reducing p53 protein levels and bypassing cellular senescence. In mouse xenograft models, shRNA-mediated *LINC00673* knockdown significantly reduced tumor growth [47,51,77] emphasizing that *LINC00673* could be a non-protein-coding key regulator of cell proliferation. Reducing its levels may delay cancer progression of early lung ADC, thereby positively influencing patient survival.

## Materials & methods

### RACE, *in vitro* translation, RNA FISH, cell fractionation and RNA stability

For 5'- and 3'-RACE analyses, the SMARTer RACE cDNA Amplification Kit (Clontech Takara Bio, Mountain View, CA, USA) was used according to the manufacturer's instructions. For first-strand cDNA synthesis, DNase I-treated total RNA from A549 cells was used. The gene-specific primers are summarized in Suppl. Table S7. The *in vitro* transcription-translation assay was based on rabbit reticulocyte extract using the TNT T7 Quick for PCR DNA kit (Promega) as described by the manufacturer. Briefly, 800 ng of gel-purified PCR products were mixed with 40  $\mu$ l of TNT T7 PCR Quick Master Mix and 3  $\mu$ l of [<sup>35</sup>S] methionine (Perkin Elmer) in a final volume of 50  $\mu$ l and the reactions were incubated for 90 min at 30°C. For SDS-PAGE, 10  $\mu$ l of each reaction were mixed with 5  $\mu$ l of SDS-Laemmli sample buffer and heated for 1 min at 90°C. The proteins were separated on a 20% SDS gel, fixed for 30 min (50% methanol and 10% acetic acid) then vacuum-dried for 1 h at 80°C. Signals were monitored by autoradiography. The primers used to generate PCR templates from plasmid DNA are listed in Suppl. Table S8. The RNA FISH probes were designed by and purchased from Stellaris (LGC Biosearch Technologies, Novato, CA, USA). For hybridization, 75 nM of probes (labeled with Quasar-670) were used and staining was performed as recommended by the manufacturer. As a negative control, the coverslips were hybridized with buffer only. The RNA FISH pictures were taken with an Olympus Cell<sup>^</sup>R microscope utilizing z-stacks and a 60x objective. All pictures of the same experiment were processed with the same settings in ImageJ, thereby using the unstained cells as a negative control to avoid signal artifacts. The cellular fractionation was carried out as previously described [78]. To estimate the half-life of *LINC00673*, A549 cells were seeded into 6-wells to reach 80% confluence one day later. For treatment, cell culture media

containing actinomycin D (10 µg/ml; Sigma-Aldrich) or the equivalent volume of DMSO (solvent control) were added to the cells. The cells were lysed in TRIzol at 0, 1, 2, 8, 16 and 24 h after treatment and the relative abundance of transcripts was determined by RT-qPCR. The respective 0 h values were used as reference and the ratios of actinomycin D-treated and DMSO solvent controls were calculated for each timepoint. The half-lives were determined by fitting the data with a non-linear least squares regression (one phase decay) with GraphPad Prism 5.

### Cellular senescence assay

5 × 10<sup>4</sup> A549 cells and 1 × 10<sup>5</sup> IMR-90 cells were grown on 60 mm dishes and the senescence-associated β-galactosidase (SA-β-Gal) activity was detected 4 days after reverse transfection. As a positive control, A549 cells were treated with 200 nM doxorubicin (Calbiochem, Merck) 12 hrs after seeding while IMR-90 cells were treated with 1 µM doxorubicin for 2 hrs at 24 hrs after seeding. Cells were washed with PBS and fixed with 0.5% glutaraldehyde in PBS for 15 min at room temperature. Then, cells were washed twice with PBS supplemented with 1 mM MgCl<sub>2</sub> (pH 6.0) for 5 min on a rocker. 2 ml X-Gal staining solution (PBS containing 1 mM MgCl<sub>2</sub>, 5 mM potassium hexacyanoferrate (III), 5 mM potassium hexacyanoferrate (II) trihydrate, 1 mg/ml X-Gal (5-bromo-4-chloro-3-indolyl-beta-D-galacto-pyranoside), pH 6.0) were added and the dishes were incubated overnight at 37° C. Next day, the cells were washed three times with distilled water and microscopy pictures were taken with the Zeiss Cell Observer using a 10x objective. For analyses, at least 200 cells were counted per condition in 3–4 independent experiments.

### Acknowledgments

The patient tissues were provided by the Lung Biobank Heidelberg, member of the Biomaterial Bank Heidelberg (BMBH), and the biobank platform of the German Center for Lung Research (DZL). We would like to thank Vladimir Benes and Tomi Ivacevic (EMBL, Heidelberg, Germany) for providing the infrastructure and support with the microarray analysis; Johanna Schott (DKFZ-ZMBH Alliance, Heidelberg, Germany) for the re-annotation of the microarray; Stefanie Grund for the cellular fractionation; Hans Johansson (LGC Biosearch Technologies) for the design of the FISH probes; the DKFZ Light Microscopy Core Facility, the ZMBH Flow Cytometry & FACS Core Facility (Heidelberg, Germany) for the technical support, the ZMBH Mass Spectrometry Core Facility for the sample preparation, technical support and data analysis. This work is part of the PhD thesis of A.R.

### Author contributions

S.D. conceived the microarray study and performed the analysis. A.W., P.A.S., T.M., M.M., H.Z. and H.H. carried out the primary tumor analysis and patient RNA isolation. M.P.S. performed the microarrays. A.R. and K. B. and S.D. designed and analyzed the experiments. A.R., K.B. and M. G. performed the experiments. O.B. and D.G. carried out experiments in ER-E2F1 cells. M.R., K.B. and F.A.M. designed, performed and analyzed retroviral infection experiments. F.A.M. provided valuable suggestions. A. R. wrote the manuscript.

### Data availability statement

The microarray data generated within this study are available at the NCBI Gene Expression Omnibus (GEO) GSE113852.

### Disclosure statement

S.D. is a co-owner of siTOOLS Biotech GmbH, Planegg/Martinsried, Germany.

### Funding

Research in the Diederichs lab is supported by the Deutsche Forschungsgemeinschaft (DFG Di 1421/7-1) and the RNA@DKFZ Cross Program Topic.

### ORCID

Sven Diederichs  <http://orcid.org/0000-0001-7901-4752>

### References

- [1] Torre LA, Bray F, Siegel RL, et al. Global cancer statistics, 2012. *CA Cancer J Clin.* 2015 Mar;65(2):87–108.
- [2] Langer CJ, Besse B, Gualberto A, et al. The evolving role of histology in the management of advanced non-small-cell lung cancer. *J Clin Oncol.* 2010 Dec 20;28(36):5311–5320.
- [3] Djebali S, Davis CA, Merkel A, et al. Landscape of transcription in human cells. *Nature.* 2012 Sep 6;489(7414):101–108.
- [4] Hangauer MJ, Vaughn IW, McManus MT. Pervasive transcription of the human genome produces thousands of previously unidentified long intergenic noncoding RNAs. *PLoS Genet.* 2013 Jun;9(6):e1003569.
- [5] Mercer TR, Dinger ME, Mattick JS. Long non-coding RNAs: insights into functions. *Nat Rev Genet.* 2009 Mar;10(3):155–159.
- [6] Yan X, Hu Z, Feng Y, et al. Comprehensive Genomic Characterization of Long Non-coding RNAs across Human Cancers. *Cancer Cell.* 2015 Oct 12;28(4):529–540.
- [7] Chen J, Wang R, Zhang K, et al. Long non-coding RNAs in non-small cell lung cancer as biomarkers and therapeutic targets. *J Cell Mol Med.* 2014 Dec;18(12):2425–2436.
- [8] Gutschner T, Diederichs S. The hallmarks of cancer: a long non-coding RNA point of view. *RNA Biol.* 2012 Jun;9(6):703–719.
- [9] Roth A, Diederichs S. Long noncoding RNAs in lung cancer. *Curr Top Microbiol Immunol.* 2016;394:57–110.
- [10] Wang KC, Chang HY. Molecular mechanisms of long noncoding RNAs. *Mol Cell.* 2011 Sep 16;43(6):904–914.
- [11] Campisi J. Aging, cellular senescence, and cancer. *Annu Rev Physiol.* 2013;75:685–705.
- [12] Cabili MN, Trapnell C, Goff L, et al. Integrative annotation of human large intergenic noncoding RNAs reveals global properties and specific subclasses. *Genes Dev.* 2011 Sep 15;25(18):1915–1927.
- [13] Li J, Han L, Roebuck P, et al. TANRIC: an interactive open platform to explore the function of lncRNAs in cancer. *Cancer Res.* 2015 Sep 15;75(18):3728–3737.
- [14] Desiere F, Deutsch EW, King NL, et al. The PeptideAtlas project. *Nucleic Acids Res.* 2006 Jan 1;34(Database issue):D655–D658.
- [15] Zhang K, Shi ZM, Chang YN, et al. The ways of action of long non-coding RNAs in cytoplasm and nucleus. *Gene.* 2014 Aug 15;547(1):1–9.
- [16] Tani H, Mizutani R, Salam KA, et al. Genome-wide determination of RNA stability reveals hundreds of short-lived noncoding transcripts in mammals. *Genome Res.* 2012 May;22(5):947–956.
- [17] Reimand J, Kull M, Peterson H, et al. g:profiler—a web-based toolset for functional profiling of gene lists from large-scale experiments. *Nucleic Acids Res.* 2007 Jul;35(Web Server issue):W193–200.
- [18] Polager S, Ginsberg D. E2F - at the crossroads of life and death. *Trends Cell Biol.* 2008 Nov;18(11):528–535.
- [19] Feldstein O, Nizri T, Doniger T, et al. The long non-coding RNA ERIC is regulated by E2F and modulates the cellular response to DNA damage. *Mol Cancer.* 2013;12(1):131.

- [20] Vernier M, Bourdeau V, Gaumont-Leclerc MF, et al. Regulation of E2Fs and senescence by PML nuclear bodies. *Genes Dev.* 2011 Jan 1;25(1):41–50.
- [21] Hannus M, Beitzinger M, Engelmann JC, et al. siPools: highly complex but accurately defined siRNA pools eliminate off-target effects. *Nucleic Acids Res.* 2014 Jul;42(12):8049–8061.
- [22] Kuilman T, Michaloglou C, Mooi WJ, et al. The essence of senescence. *Genes Dev.* 2010 Nov 15;24(22):2463–2479.
- [23] Campisi J, d'Adda Di Fagagna F. Cellular senescence: when bad things happen to good cells. *Nat Rev Mol Cell Biol.* 2007 Sep;8(9):729–740.
- [24] Tanaka H, Fujii Y, Hirabayashi H, et al. Disruption of the RB pathway and cell-proliferative activity in non-small-cell lung cancers. *Int J Cancer J Inter Du Cancer.* 1998 Apr 17;79(2):111–115.
- [25] Kashiwabara K, Oyama T, Sano T, et al. Correlation between methylation status of the p16/CDKN2 gene and the expression of p16 and Rb proteins in primary non-small cell lung cancers. *Int J Cancer J Inter Du Cancer.* 1998 Jun 19;79(3):215–220.
- [26] Mogi A, Kuwano H. TP53 mutations in nonsmall cell lung cancer. *J Biomed Biotechnol.* 2011;2011:583929.
- [27] Althubiti M, Lezina L, Carrera S, et al. Characterization of novel markers of senescence and their prognostic potential in cancer. *Cell Death Dis.* 2014;5:e1528.
- [28] Dimri GP, Lee X, Basile G, et al. A biomarker that identifies senescent human cells in culture and in aging skin in vivo. *Proc Natl Acad Sci U S A.* 1995 Sep 26;92(20):9363–9367.
- [29] Frolov MV, Dyson NJ. Molecular mechanisms of E2F-dependent activation and pRB-mediated repression. *J Cell Sci.* 2004 May 1;117(Pt 11):2173–2181.
- [30] Chicas A, Wang X, Zhang C, et al. Dissecting the unique role of the retinoblastoma tumor suppressor during cellular senescence. *Cancer Cell.* 2010 Apr 13;17(4):376–387.
- [31] Chen T, Xue L, Niu J, et al. The retinoblastoma protein selectively represses E2F1 targets via a TAAC DNA element during cellular senescence. *J Biol Chem.* 2012 Oct 26;287(44):37540–37551.
- [32] Narita M, Nunez S, Heard E, et al. Rb-mediated heterochromatin formation and silencing of E2F target genes during cellular senescence. *Cell.* 2003 Jun 13;113(6):703–716.
- [33] Coppe JP, Desprez PY, Krtolica A, et al. The senescence-associated secretory phenotype: the dark side of tumor suppression. *Annu Rev Pathol.* 2010;5:99–118.
- [34] Bartkova J, Rezaei N, Liontos M, et al. Oncogene-induced senescence is part of the tumorigenesis barrier imposed by DNA damage checkpoints. *Nature.* 2006 Nov 30;444(7119):633–637.
- [35] Di Micco R, Fumagalli M, Cicalese A, et al. Oncogene-induced senescence is a DNA damage response triggered by DNA hyper-replication. *Nature.* 2006 Nov 30;444(7119):638–642.
- [36] Mallette FA, Gaumont-Leclerc MF, Ferbeyre G. The DNA damage signaling pathway is a critical mediator of oncogene-induced senescence. *Genes Dev.* 2007 Jan 1;21(1):43–48.
- [37] Park C, Lee I, Kang WK. E2F-1 is a critical modulator of cellular senescence in human cancer. *Int J Mol Med.* 2006 May;17(5):715–720.
- [38] Schubert S, Shannon K, Bollag G. Hyperactive Ras in developmental disorders and cancer. *Nat Rev Cancer.* 2007 Apr;7(4):295–308.
- [39] Serrano M, Lin AW, McCurrach ME, et al. Oncogenic ras provokes premature cell senescence associated with accumulation of p53 and p16INK4a. *Cell.* 1997 Mar 7;88(5):593–602.
- [40] Mallette FA, Goumard S, Gaumont-Leclerc MF, et al. Human fibroblasts require the Rb family of tumor suppressors, but not p53, for PML-induced senescence. *Oncogene.* 2004 Jan 8;23(1):91–99.
- [41] Kortlever RM, Higgins PJ, Bernards R. Plasminogen activator inhibitor-1 is a critical downstream target of p53 in the induction of replicative senescence. *Nat Cell Biol.* 2006 8;Aug(8):877–884.
- [42] Roy N, Stoyanova T, Dominguez-Brauer C, et al. DDB2, an essential mediator of premature senescence. *Mol Cell Biol.* 2010 Jun;30(11):2681–2692.
- [43] Guan D, Factor D, Liu Y, et al. The epigenetic regulator UHRF1 promotes ubiquitination-mediated degradation of the tumor-suppressor protein promyelocytic leukemia protein. *Oncogene.* 2013 Aug 15;32(33):3819–3828.
- [44] Mason DX, Jackson TJ, Lin AW. Molecular signature of oncogenic ras-induced senescence. *Oncogene.* 2004 Dec 9;23(57):9238–9246.
- [45] Abdelmohsen K, Panda AC, Kang MJ, et al. 7SL RNA represses p53 translation by competing with HuR. *Nucleic Acids Res.* 2014 Sep;42(15):10099–10111.
- [46] White NM, Cabanski CR, Silva-Fisher JM, et al. Transcriptome sequencing reveals altered long intergenic non-coding RNAs in lung cancer. *Genome Biol.* 2014;15(8):429.
- [47] Shi X, Ma C, Zhu Q, et al. Upregulation of long intergenic noncoding RNA 00673 promotes tumor proliferation via LSD1 interaction and repression of NCALD in non-small-cell lung cancer. *Oncotarget.* 2016 May 3;7(18):25558–25575.
- [48] Lu W, Zhang H, Niu Y, et al. Long non-coding RNA linc00673 regulated non-small cell lung cancer proliferation, migration, invasion and epithelial mesenchymal transition by sponging miR-150-5p. *Mol Cancer.* 2017 Jul 11;16(1):118.
- [49] Schmidt K, Joyce CE, Buquicchio F, et al. The lncRNA SLNCR1 mediates melanoma invasion through a conserved SRA1-like region. *Cell Rep.* 2016 May 31;15(9):2025–2037.
- [50] Yu J, Liu Y, Gong Z, et al. Overexpression long non-coding RNA LINC00673 is associated with poor prognosis and promotes invasion and metastasis in tongue squamous cell carcinoma. *Oncotarget.* 2017 Mar 7;8(10):16621–16632.
- [51] Huang M, Hou J, Wang Y, et al. Long noncoding RNA LINC00673 Is activated by SP1 and exerts oncogenic properties by interacting with LSD1 and EZH2 in gastric cancer. *Mol ther.* 2017 Apr 5;25(4):1014–1026.
- [52] Ba MC, Long H, Cui SZ, et al. Long noncoding RNA LINC00673 epigenetically suppresses KLF4 by interacting with EZH2 and DNMT1 in gastric cancer. *Oncotarget.* 2017 Nov 10;8(56):95542–95553.
- [53] Berteaux N, Lottin S, Monte D, et al. H19 mRNA-like noncoding RNA promotes breast cancer cell proliferation through positive control by E2F1. *J Biol Chem.* 2005 Aug 19;280(33):29625–29636.
- [54] Wan G, Mathur R, Hu X, et al. Long non-coding RNA ANRIL (CDKN2B-AS) is induced by the ATM-E2F1 signaling pathway. *Cell Signal.* 2013 May;25(5):1086–1095.
- [55] Bida O, Gidoni M, Ideses D, et al. A novel mitosis-associated lncRNA, MA-linc1, is required for cell cycle progression and sensitizes cancer cells to Paclitaxel. *Oncotarget.* 2015 Sep 29;6(29):27880–27890.
- [56] Zhang E, Yin D, Han L, et al. E2F1-induced upregulation of long noncoding RNA LINC00668 predicts a poor prognosis of gastric cancer and promotes cell proliferation through epigenetically silencing of CKIs. *Oncotarget.* 2016 Apr 26;7(17):23212–23226.
- [57] Polager S, Ginsberg D. p53 and E2f: partners in life and death. *Nat Rev Cancer.* 2009 Oct;9(10):738–748.
- [58] Laine A, Westermarck J. Molecular pathways: harnessing E2F1 regulation for pro-senescence therapy in p53-defective cancer cells. *Clin Cancer Res off J Am Assoc Cancer Res.* 2014 Jul 15;20(14):3644–3650.
- [59] Young AP, Nagarajan R, Longmore GD. Mechanisms of transcriptional regulation by Rb-E2F segregate by biological pathway. *Oncogene.* 2003 Oct 16;22(46):7209–7217.
- [60] Braig M, Lee S, Loddenkemper C, et al. Oncogene-induced senescence as an initial barrier in lymphoma development. *Nature.* 2005 Aug 4;436(7051):660–665.
- [61] Chen Z, Trotman LC, Shaffer D, et al. Crucial role of p53-dependent cellular senescence in suppression of Pten-deficient tumorigenesis. *Nature.* 2005 Aug 4;436(7051):725–730.
- [62] Collado M, Gil J, Efeyan A, et al. Tumour biology: senescence in premalignant tumours. *Nature.* 2005 Aug 4;436(7051):642.
- [63] Michaloglou C, Vredeveld LC, Soengas MS, et al. BRAFE600-associated senescence-like cell cycle arrest of human naevi. *Nature.* 2005 Aug 4;436(7051):720–724.
- [64] Lazorthes S, Vallot C, Briois S, et al. A vlinRNA participates in senescence maintenance by relieving H2AZ-mediated repression at the INK4 locus. *Nat Commun.* 2015;6:5971.
- [65] Abdelmohsen K, Gorospe M. Noncoding RNA control of cellular senescence. *Wiley Interdiscip Rev RNA.* 2015 Nov;6(6):615–629.

- [66] Montes M, Lund AH. Emerging roles of lncRNAs in senescence. *FEBS J.* 2016 Jul;283(13):2414–2426.
- [67] Zheng J, Huang X, Tan W, et al. Pancreatic cancer risk variant in LINC00673 creates a miR-1231 binding site and interferes with PTPN11 degradation. *Nat Genet.* 2016 May 23;48:747–757.
- [68] Kapic A, Helmbold H, Reimer R, et al. Cooperation between p53 and p130(Rb2) in induction of cellular senescence. *Cell Death Differ.* 2006 Feb;13(2):324–334.
- [69] Tay Y, Rinn J, Pandolfi PP. The multilayered complexity of ceRNA crosstalk and competition. *Nature.* 2014 Jan 16;505(7483):344–352.
- [70] Faghihi MA, Modarresi F, Khalil AM, et al. Expression of a noncoding RNA is elevated in Alzheimer's disease and drives rapid feed-forward regulation of beta-secretase. *Nat Med.* 2008 Jul;14(7):723–730.
- [71] Kretz M, Siprashvili Z, Chu C, et al. Control of somatic tissue differentiation by the long non-coding RNA TINCR. *Nature.* 2013 Jan 10;493(7431):231–235.
- [72] Gong C, Maquat LE. lncRNAs transactivate STAU1-mediated mRNA decay by duplexing with 3' UTRs via Alu elements. *Nature.* 2011 Feb 10;470(7333):284–288.
- [73] Liu X, Li D, Zhang W, et al. Long non-coding RNA gadd7 interacts with TDP-43 and regulates Cdk6 mRNA decay. *Embo J.* 2012 Nov 28;31(23):4415–4427.
- [74] Carrieri C, Cimatti L, Biagioli M, et al. Long non-coding antisense RNA controls Uchl1 translation through an embedded SINEB2 repeat. *Nature.* 2012 Nov 15;491(7424):454–457.
- [75] Yoon JH, Abdelmohsen K, Srikantan S, et al. lincRNA-p21 suppresses target mRNA translation. *Mol Cell.* 2012 Aug 24;47(4):648–655.
- [76] Gumireddy K, Li A, Yan J, et al. Identification of a long non-coding RNA-associated RNP complex regulating metastasis at the translational step. *Embo J.* 2013 Oct 16;32(20):2672–2684.
- [77] Ma C, Wu G, Zhu Q, et al. Long intergenic noncoding RNA 00673 promotes non-small-cell lung cancer metastasis by binding with EZH2 and causing epigenetic silencing of HOXA5. *Oncotarget.* 2017 May 16;8(20):32696–32705.
- [78] Grund SE, Polycarpou-Schwarz M, Luo C, et al. Rare Drosha splice variants are deficient in microRNA processing but do not affect general microRNA expression in cancer cells. *Neoplasia.* 2012 Mar;14(3):238–248.